

## Passive magnetic coil design for electromagnetic interference evaluation of axle counters

Yoppy<sup>1</sup>, Yudhistira<sup>1</sup>, Hutomo Wahyu Nugroho<sup>1</sup>, Elvina Trivida<sup>1</sup>, Tyas Ari Wahyu Wijanarko<sup>1,2</sup>,  
Aditia Nur Bakti<sup>1</sup>, Dwi Mandaris<sup>1</sup>

<sup>1</sup>Research Center for Testing Technology and Standards, National Research and Innovation Agency, South Tangerang, Indonesia

<sup>2</sup>School of Electrical Engineering and Informatics, Bandung Institute of Technology, Bandung, Indonesia

### Article Info

#### Article history:

Received May 24, 2023

Revised Aug 18, 2023

Accepted Sep 6, 2023

#### Keywords:

Axle counters

Electromagnetic compatibility

EN 50592

Measurement sensitivity

Passive magnetic coil

### ABSTRACT

Measurement of magnetic fields near the railway tracks is crucial to ensure compatibility with the operation of axle counters. According to EN 50592 standard, the magnetic field is detected with a passive magnetic coil and an oscilloscope. From previous studies, in general, there has been no in-depth analysis of how the choice of coil winding parameters could affect the coil output voltage, which then affect the measurement sensitivity, in particular the coil design based on the standard and its applicability for electromagnetic interference (EMI) evaluation of axle counters. Therefore, this paper will explore the design of a passive magnetic coil to obtain the optimum coil output voltage within the frequency range. Simulations showed that for 10-100 kHz and 100 kHz–1.3 MHz range, the optimum number of turns happened at 60-100 and 15-60 turns, respectively. Based on that, two example coils had been built. Simulations and measurements of their frequency response were in good agreement, with a deviation less than 1.0 dB.

*This is an open access article under the [CC BY-SA](https://creativecommons.org/licenses/by-sa/4.0/) license.*



### Corresponding Author:

Yoppy

Research Center for Testing Technology and Standards, National Research and Innovation Agency

South Tangerang, Banten, Indonesia

Email: yoppy.chia@gmail.com

## 1. INTRODUCTION

Electromagnetic (EM) noises in the railway environment have shown a considerable increase with the increasing application of power electronic and semiconductor devices in railcars, radio-based communication systems, and magnetic braking systems [1]. These noise sources have the potential to impact the trackside signaling equipment, such as axle counters, track circuits, wheel detectors, and potentially compromising their safety and performance. To ensure that rolling stock is compatible with axle counting systems, it is essential to measure emissions from the vehicles to demonstrate this compatibility [2]. The emissions, caused by the vehicles, are measured as magnetic fields in X, Y, and Z directions. The measurements are conducted using a standardized magnetic coil with dimensions of 15 cm in length, 5 cm in width, and 5 cm in height, as specified in the EN 50592 standard [2]. Although the coil area is predetermined, the standard allows for flexibility in determining the number of turns, wire diameters, inter-turn spacing, and the number of layers. These parameters will definitely affect the coil output voltage to a certain degree, and it is interesting to investigate these effects in more detail to see if there is any specific configuration that is more optimum in terms of good sensitivity.

The magnetic coil sensors are used in variety of applications, from identifying the microstructural condition of steel alloys [3] to their use in geophysical techniques for groundwater exploration [4].

Additionally, several studies utilizing measurements and simulations have been performed on railway axle counters [5]–[7]. However, generally, these studies have not described into how selecting different coil winding parameters could affect the coil's output voltage and subsequently, the measurement sensitivity. In fact, the winding configurations determined the coil impedance, and it will interact with both the cable impedance and the oscilloscope impedance, eventually affecting the voltage measured at the oscilloscope. Moreover, there are very few previous research on developed magnetic coil specifically for detecting electromagnetic interference (EMI) from axle counter based on [2]. Therefore, this paper focuses on exploring magnetic coil design on the effect of various parameter configurations to the coil output voltage which applicable for measuring noises generated from the axle counters and the rolling stock.

## 2. PASSIVE MAGNETIC COIL

A passive magnetic coil could be used as a receiving antenna or as a probe to measure magnetic flux density [8]. A conceptual geometry of the rectangular multturn loop antenna in a receiving mode with  $N$  turns is shown in Figure 1. When an electromagnetic plane wave propagates toward the coil with the incident angle of  $\theta$ , an open-circuit voltage ( $V_{OC}$ ) arises, which are influenced by several factors such as the number of turns ( $N$ ), frequency ( $f$ ), magnetic field permeability ( $\mu_0$ ) and magnetic field density ( $H$ ) penetrating the loop area [9]–[11]. The relation is formulated in (1).

$$V_{OC} = 2\pi f a b N \mu_0 H \sin\theta \quad (1)$$

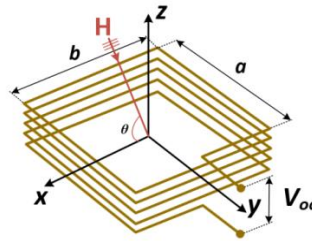


Figure 1. Magnetic coil cross-sectional model as a loop antenna [11]

Basically, a higher output voltage is more desirable because it will be more readable to the measuring instrument, such as an oscilloscope. Given that the coil area is fixed as governed by the standard, based on (1) increasing the number of turns ( $N$ ) may seem to be the easiest way to obtain a higher output voltage. However, increasing the number of turns also increases the coil impedance, which will interact with the measuring instrument's impedance. At a certain point, increasing the number of turns may actually reduce the voltage read by the instrument due to an increase of the coil impedance.

The coil impedance is frequency-dependent and is contributed by the resistance, inductance, and capacitance of the coil. Based on the IEC 60287-1-1 standard, the alternating current (AC) resistance ( $R_{AC}$ ) of a conducting wire can be calculated from its direct current (DC) resistance ( $R_{DC}$ ) [12] as formulated in (2), where the additional factor  $y_s$  is due to skin effects. However, the formula is found to be accurate only for a single wire without neighboring wires as in a coil [12]. Because of neighboring wires, the resistance of a magnetic coil would increase due to both the skin effect and proximity effect.

$$R_{AC} = R_{DC}(1 + y_s) \quad (2)$$

Meanwhile, the coil inductance value is greatly influenced by the length, dimensions, and number of turns of the coil. The inductance could be calculated by using Niwa's formula [13], [14]. As for the capacitance, there are numerous papers discuss the method to compute the capacitance of a tubular coil [15]–[19], [20]–[24]. However, there have not been found a suitable method to determine the capacitance of a rectangular coil. Therefore, capacitance is excluded in the calculation, and it also will be shown in the next section that the exclusion of capacitance is acceptable in the frequency of interest.

On the other hand, there is a tool named FastHenry2, which is a free EM simulation tool for computing the frequency-dependent self and mutual inductances and resistances of a 3D conductive structure, in the magnetoquasistatic approximation [25]. The 3D structure in FastHenry2 is defined in a text-based fashion. Moreover, FastHenry2 can be automated from other programming tools, such as Python. In this paper, FastHenry2 is used in conjunction with Python to fully automate the definition of coil structures,

to run the EM solver, and to extract the inductances and resistances of numerous coil winding configurations.

In the electromagnetic compatibility (EMC) measurement of axle counters, a magnetic coil having an internal impedance  $Z_{in}$  is connected to an oscilloscope having impedance  $Z_L$  via a coaxial cable with a characteristic impedance  $Z_0$  as shown in Figure 2(a). The existence of impedance  $Z_{in}$ ,  $Z_0$ , and  $Z_L$  influences the output voltage ( $V_{out}$ ) measured at the oscilloscope. Therefore, simply increasing the number of turns ( $N$ ) will not always increase the output voltage.

Looking from the coil into the transmission cable, Figure 2(a) can be simplified into Figure 2(b). Mathematically, the equation for determining  $V_{out}$  is shown in (3) where  $\beta$  is a wavenumber ( $2\pi f/v$ ),  $l$  is the length of cable, and  $\Gamma$  is a reflection coefficient [26]. If the values of cable impedance  $Z_0$  and instrument impedance  $Z_L$  are equal, the value of  $\Gamma$  will be zero so that (3) can be further simplified to (6).

$$V_{out} = \frac{Z_{eq} V_{oc}}{Z_{in} + Z_{eq}} \frac{1}{(e^{j\beta l} + \Gamma e^{-j\beta l})} \quad (3)$$

where,

$$\Gamma = \frac{Z_L - Z_0}{Z_L + Z_0} \quad (4)$$

$$Z_{eq} = Z_0 \frac{Z_L + jZ_0 \tan\beta l}{Z_0 + jZ_L \tan\beta l} \quad (5)$$

$$V_{out} = \frac{Z_{eq} V_{oc}}{Z_{in} + Z_{eq}} \frac{1}{(e^{j\beta l})} \quad (6)$$

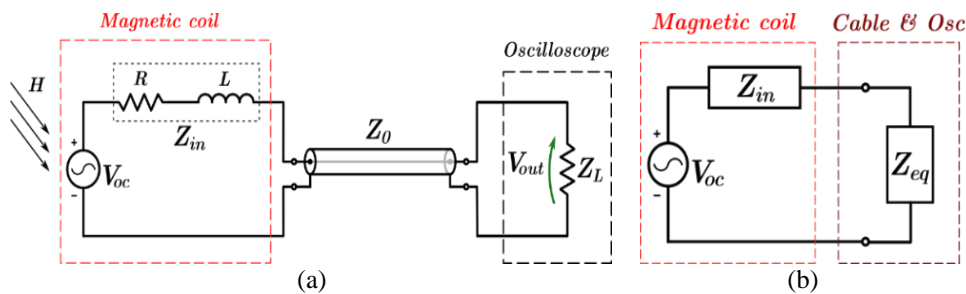


Figure 2. Electrical schematic of the coil's output voltage measurement setup: (a) in its full form and (b) in a simplified form

### 3. SIMULATION AND MEASUREMENT METHODS

A coil impedance is frequency-dependent, and its length, dimensions, wire diameter, and number of turns collectively determine the coil resistance and reactance. In this paper, a tool called FastHenry2 is used to compute the resistances and inductances of various coil winding configurations [25]. The extracted resistances and inductances are then used to calculate the coil impedance.

The number of layers was kept constant at a single layer. The winding was assumed tightly wound such that the inter-turn spacing was solely due to the enamel thickness, and it was kept fixed at 0.06 mm. The number of turns was varied from 2-100, whereas the wire cross-section was 0.3-0.9 mm. In FastHenry2, the wire of the coil could only be modelled as a rectangular shape, whereas in the actual coil a cylindrical wire was used. Due to this difference, the discrepancy between simulation and measurement results is expected. The discretization of segments in FastHenry2 was set to  $nhinc = 2$  and  $nwinc = 2$ .

The next step was to run circuit simulations based on Figure 2 to obtain the  $V_{out}$ . The simulation was done in Octave by feeding all the coil resistances and inductances resulting from FastHenry2 along with cable properties and instrument impedance into (6). The magnetic coil dimension is referred to [2], and the frequency range was 10 kHz-1.3 MHz. A velocity factor of 66% was used in the simulation. It is referred to the RG58A/U cable datasheet [27], and was confirmed with a wave reflection measurement on the actual cable.

After performing the above simulations, the results were evaluated and optimal configurations of wire diameters and number of turns was decided. The next step was to fabricate prototypes of the magnetic coil with their respective specifications for lower frequency (LF) and higher frequency (HF) measurements.

The performance of the constructed coils was measured in a gigahertz transverse electromagnetic cell (GTEM). Figure 3 shows the measurement setup of the coil. The coil was placed inside the GTEM and the door was fully closed. The distance between the bottom and the septum of the GTEM was 0.53 m. In addition, the RG58A/U coaxial cable used in the measurement has a typical attenuation of 0.5 dB/100 feet @ 1 Mhz. The cable length was 7.6 m, and an attenuation of 0.12 dB is expected. Both the coaxial cable and the measuring instrument's input impedance are matched at 50 ohms to avoid signal resonance. The frequency response of the constructed coils was measured from 10 kHz to 1.3 MHz, and the measurement results were compared with the simulation results.

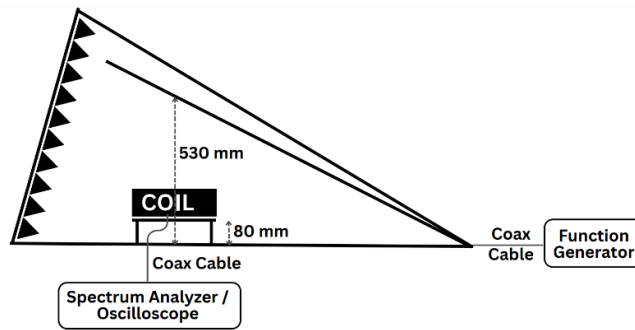


Figure 3. Coil measurement in GTEM

#### 4. SIMULATION RESULTS

A comprehensive simulation had been done to evaluate the effect of coil wire diameters and the number of turns on the  $V_{out}$ . The simulation was based on the circuit schematic in Figure 2. A magnetic field of  $H=120 \text{ dB}\mu\text{A/m}$  was simulated to perpendicularly impinge the coil cross-section. The cable impedance and oscilloscope impedance were set equal to  $50 \Omega$ .

As recommended by the standard [2], measurement is done in the low frequency and high frequency range, which are 10-100 kHz and 100 kHz-1.3 MHz, respectively. Due to a large number of data, three border frequencies, e.g., 10 kHz, 100 kHz, and 1.3 MHz were chosen as representative points of observation from the whole frequency range. As shown in Figure 4, in general  $V_{out}$  increases with wire diameter for both coil  $15 \times 5 \text{ cm}^2$  as shown in Figure 4(a) and coil  $5 \times 5 \text{ cm}^2$  as shown in Figure 4(b). This can be explained by the fact that larger wire will have both lower resistance and inductance, and thus lower coil impedance. However, an oversize wire might cause difficulties in constructing the coil, for example, a 0.9 mm wire diameter could be inconvenient to wind. Additionally, the larger wire would also result in a longer coil, whereas its total length should fit in the bobbin's length.

On the other hand, the number of turns has more significant and interesting effects on  $V_{out}$ . The most striking feature from Figure 4 is that at a number of turns around 4-8, at 1.3 MHz  $V_{out}$  reaches a maximum which is desirable in order to obtain a good measurement result by the oscilloscope. However, the downside is that there is a wide discrepancy compared to  $V_{out}$  at 100 kHz. Due to in actual measurement  $V_{out}$  is measured using an oscilloscope having limited dynamic range (volt/div), large differences of  $V_{out}$  between that of high and low frequencies would result in accuracy loss at low frequency parts.

For instance, a  $15 \times 5 \text{ cm}$  coil using wire diameter 0.5 mm with 5 turns will give  $V_{out}$  on a  $50 \Omega$  oscilloscope  $235 \text{ mV}_{rms}$  and  $25 \text{ mV}_{rms}$  at frequency 1.3 MHz and 100 kHz respectively when exposed under a magnetic field  $H=120 \text{ dB}\mu\text{A/m}$ . It means that the signal at 100 kHz would experience a worse resolution. Meanwhile, an oscilloscope display range setting of at least  $235 \text{ mV}_{rms} \times \sqrt{2} \times 2 = 664 \text{ mV}_{pp}$  is required to prevent clipping of the maximum expected signal. If the oscilloscope is using a common 8-bit analog to digital converter (ADC), then the resolution is  $664 \text{ mV}/256=2.59 \text{ mV}$ . Therefore, the signal at 100 kHz would experience a resolution of  $2.59 \text{ mV}/(25 \text{ mV}_{rms} \times \sqrt{2} \times 2)=3.66\%$  of it is maximum expected signal, which is quite coarse.

Another important observation from Figure 4 is that there is no single best coil configuration. Rather, it is a matter of trade-off between two aspects: i)  $V_{out}$  discrepancy between high and low frequency, and ii) magnitude of  $V_{out}$ . At a high number of turns,  $V_{out}$  discrepancy between high and low frequency is converging, which is desirable; however, it resulted a lower magnitude of  $V_{out}$ . Therefore, for 100 kHz-1.3 MHz measurement, a balance of the two aspects can be considered to happen at a range of 15-60 turns. Whereas for 10-100 kHz measurement, 60-100 turns could be a good choice to achieve the balance.

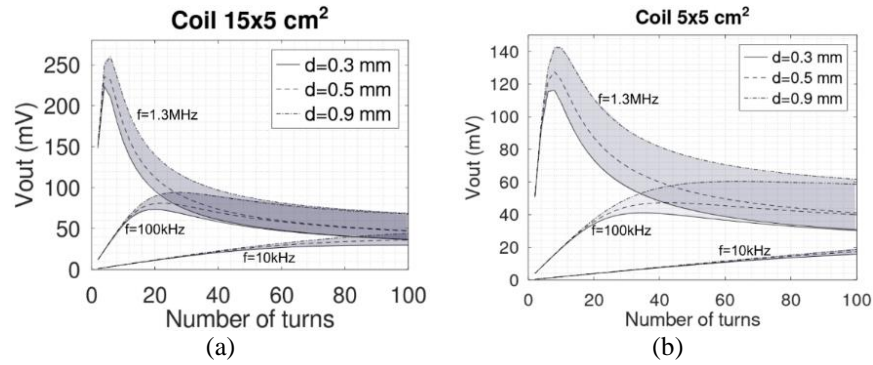


Figure 4.  $V_{out}$  at 10 kHz, 100 kHz, and 1.3 MHz due to variation of number of turns and wire diameters for (a) Coil  $15 \times 5 \text{ cm}^2$  and (b) Coil  $5 \times 5 \text{ cm}^2$

## 5. MEASUREMENT RESULTS

Based on the finding discussed above, two example coils had been built with the following parameters shown in Table 1. The coils were wound on a 3D printed hollow plastic block as shown in Figure 5. Figure 5(a) shows the constructed high frequency coil, while and Figure 5(b) depicts the low frequency. The enamelled copper wire was tightly wound such that the inter-turn spacing was solely due to the thickness of the enamel. The number of layers was kept at a single layer.

Table 1. Parameters of coil winding

	Coil area ( $\text{cm}^2$ )	Number of turns	Wire diameter (mm)	Inter-turn spacing (mm)
LF Coils (10-100 kHz)	$5 \times 5$	60	0.3	0.06
HF Coils (100 kHz-1.3 MHz)	$15 \times 5$	20	0.3	0.06



Figure 5. The constructed coils of (a) high frequency and (b) low frequency

### 5.1. Coil inductance and resistance

The inductance and resistance of the constructed coils were measured using inductance-capacitance-resistance (LCR) meter Agilent E4980AL. Measurement results were compared with those computed in FastHenry2, as shown in Table 2. The discrepancy in resistance was due to the rectangular cross-section conductor assumed in FastHenry2 whereas the actual wire cross-section was circular. In FastHenry2, a circular cross-section wire with diameter  $D$  was approximated with a rectangular one with a dimension of  $D \times D$ . As a result, the circular wire which had a smaller cross-section area would show higher resistance than that of FastHenry2. In DC, the resistance ratio between measurement and FastHenry2 would be (7). As a result, the measured and computed inductances were in close agreement. Inductances were less sensitive to the wire cross-section area.

$$\frac{R_{meas.}}{R_{FH2}} = \frac{R_{circ}}{R_{rect}} = \frac{D^2}{\frac{(\pi D^2)}{4}} = 4/\pi = 1.27 \quad (7)$$

Table 2. Comparison of measured and computed inductance and resistance

Test frequency (kHz)	Coil Area (cm <sup>2</sup> )	Number of turns	Inductance			Resistance		
			Meas (μH)	FH2 (μH)	Meas/FH2	Meas (μH)	FH2 (μH)	Meas/FH2
10	5×5	60	242.6	243.4	0.99	2.98	2.30	1.29
	5×15	60	599.8	591.3	1.01	5.95	4.60	1.29
300	5×5	20	44.3	42.3	1.05	1.56	1.16	1.35
	5×15	20	100.3	98.2	1.02	2.97	2.35	1.26

**5.2. Coil’s frequency response**

Measurements were done to characterize the frequency response of the constructed coils. The coils were exposed with a magnetic field in a GTEM as shown in Figure 3. A high-power radio frequency (RF) amplifier was required to generate a magnetic field of 120 dBμA/m of the standard limit. Because such an amplifier was not available in the lab, a signal generator with an output of 120 dBμV was directly fed to the GTEM. Due to small magnitude signal, instead of an oscilloscope, a spectrum analyzer (Rigol DSA815) was used to measure the coil output voltage. Although the actual application in the field is using an oscilloscope and a higher magnetic field is expected, and the frequency response obtained in this measurement will also be valid for its case because the coil and cabling are linear systems.

Figure 6 depicts the frequency response of low frequency (LF) coils. The frequency of interest is 10-100 kHz, but frequency above 100 kHz is shown for extended evaluation. In general, the measurement and simulation results were in good agreement, with a deviation less than 1.0 dB. The frequency response of the constructed high frequency (HF) coils is shown in Figure 7. The frequency of interest is 100 kHz - 1.3 MHz, but frequency below 100 kHz is included as a complemented. Generally, the measurement and simulation results were also well aligned, with a difference of less than 0.3 dB.

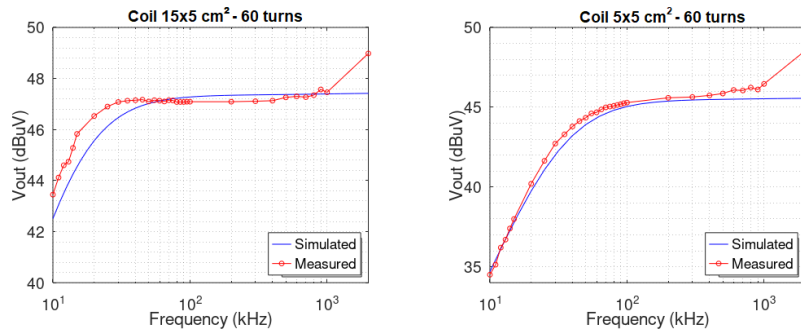


Figure 6. Frequency response of LF coils

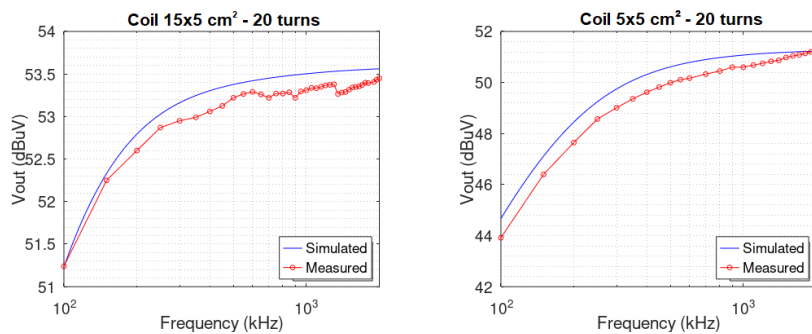


Figure 7. Frequency response of HF coils

**6. CONCLUSION**

Simulation results showed that output voltage  $V_{out}$  did not always increase with adding more turns. Due to the impedance of the coil, at some point  $V_{out}$  become lower as the number of turns was increasing. For 10-100 kHz measurement, the optimum number of turns could be considered at a range of 60-100. Whereas for 100 kHz-1.3 MHz measurement, it was 15-60 turns.

Based on the findings above, two example coils had been built using a 3D printed hollow plastic block. Measurements were done to characterize the frequency response of the constructed coils. In general, for the 10-100 kHz range, the frequency response of measurement and simulation results were in good agreement, with a deviation less than 1.0 dB. In the higher frequency band, 100 kHz-1.3 MHz, the results were also well aligned, with less than 0.3 dB discrepancies. Based on this analysis, the magnetic coil sensor prototype can be used appropriately to evaluate the electromagnetic field emission of the axle counter based on the standard technique. Moreover, the sensor can still be developed further for more accurate measurement.

## ACKNOWLEDGEMENTS

The authors would like to thank and highly appreciate PT. INKA (Persero) and PT. KAI for the financial support as well as the opportunity to design and develop the magnetic coil sensors.

## REFERENCES

- [1] A. Zamani and A. Mirabadi, "Optimization of sensor orientation in railway wheel detector, using kriging method," *Journal of Electromagnetic Analysis and Applications*, vol. 03, no. 12, pp. 529–536, 2011, doi: 10.4236/jemaa.2011.312080.
- [2] "BS EN 50592:2016-Railway applications-testing of rolling stock for electromagnetic compatibility with axle counters," BSI Standards Institution, 2016.
- [3] A. Leonhardt, F. Wendler, R. Wertheim, V. Kräusel, and O. Kanoun, "Induction coil as sensor for contactless, continuous in-process determination of steel microstructure by means of magnetic induction spectroscopy (MIS)," *CIRP Journal of Manufacturing Science and Technology*, vol. 33, pp. 240–246, May 2021, doi: 10.1016/j.cirpj.2021.03.011.
- [4] T. Lin, S. Li, M. Wang, and Y. Zhang, "Acquisition and correction for early surface nuclear magnetic resonance signal based on multi-turn small air-core coil sensors," *Measurement*, vol. 216, Jul. 2023, doi: 10.1016/j.measurement.2023.112902.
- [5] D. Adamski, K. Ortel, and J. Furman, "Research on measurement of electromagnetic fields generated by electric and combustion powered rolling stock," *MATEC Web of Conferences*, vol. 294, Oct. 2019, doi: 10.1051/mateconf/201929403016.
- [6] R. D. Persichini, D. Di Febo, V. Cala, C. Malta, and A. Orlandi, "EMC analysis of axle counters in the Italian railway network," *IEEE Transactions on Electromagnetic Compatibility*, vol. 57, no. 1, pp. 44–51, Feb. 2015, doi: 10.1109/TEM.2014.2360065.
- [7] V. Kasik and M. Tutsch, "Simulation and measurement of axle counter with FPGA," *Department of Cybernetics and Biomedical Engineering, Technical University of Ostrava*, 2012.
- [8] C. A. Balanis, *Antenna theory: analysis and design*, 4th ed. John Wiley and Sons, 2016.
- [9] W. G. Fano, "Standard electric and magnetic field for calibration," in *Electric Field*, InTech, 2018.
- [10] G. I. Quintana, R. Alonso, and W. G. Fano, "Loop antenna characterization for ELF and SLF measurements," *Elektron*, vol. 2, no. 2, pp. 95–100, Dec. 2018, doi: 10.37537/rev.elektron.2.2.45.2018.
- [11] S. Youn, T. H. Lim, E. Kang, D. H. Lee, K. B. Kim, and H. Choo, "Design of a miniaturized rectangular multilayer loop antenna for shielding effectiveness measurement," *Sensors*, vol. 20, no. 11, Jun. 2020, doi: 10.3390/s20113178.
- [12] J.-R. Riba, "Analysis of formulas to calculate the AC resistance of different conductors' configurations," *Electric Power Systems Research*, vol. 127, pp. 93–100, Oct. 2015, doi: 10.1016/j.epsr.2015.05.023.
- [13] Y. Niwa, "On the calculation of self inductance of coils wound on square forms," *The Journal of the Institute of Electrical Engineers of Japan*, vol. 43, no. 425, pp. 958–976, 1923.
- [14] H. Nagaoka, "The inductance coefficients of solenoids," *The journal of the College of Science, Imperial University of Tokyo, Japan*, vol. 27, pp. 1–33, 1909.
- [15] A. Ayachit and M. K. Kazimierzuk, "Self-capacitance of single-layer inductors with separation between conductor turns," *IEEE Transactions on Electromagnetic Compatibility*, vol. 59, no. 5, pp. 1642–1645, Oct. 2017, doi: 10.1109/TEM.2017.2681578.
- [16] G. Grandi, M. K. Kazimierzuk, A. Massarini, and U. Reggiani, "Stray capacitances of single-layer solenoid air-core inductors," *IEEE Transactions on Industry Applications*, vol. 35, no. 5, pp. 1162–1168, 1999, doi: 10.1109/28.793378.
- [17] D. W. Knight, "The self-resonance and self-capacitance of solenoid coils: Applicable theory, models and calculation methods," *G3YNH info*, vol. 10, 2016.
- [18] A. Mariscotti, "Determination of the stray capacitance of single layer solenoids," in *2011 IEEE International Instrumentation and Measurement Technology Conference*, May 2011, pp. 1–5, doi: 10.1109/IMTC.2011.5944057.
- [19] Q. Yu and T. W. Holmes, "Stray capacitance modeling of inductors by using the finite element method," in *IEEE International Symposium on Electromagnetic Compatibility. Symposium Record*, 1999, vol. 1, pp. 305–310, doi: 10.1109/ISEMC.1999.812918.
- [20] A. De Leo and G. Cerri, "A charge distribution based model for the evaluation of an air-coil stray capacitance," *IEEE Transactions on Electromagnetic Compatibility*, vol. 61, no. 5, pp. 1673–1677, Oct. 2019, doi: 10.1109/TEM.2018.2870744.
- [21] M.-X. Du, Y. Zhang, H. Wang, Y. Tian, Z. Ouyang, and K.-X. Wei, "An improved calculation method for static capacitance in inductor windings," *Progress In Electromagnetics Research C*, vol. 104, pp. 25–36, 2020, doi: 10.2528/PIERC20051203.
- [22] A. Massarini and M. K. Kazimierzuk, "Self-capacitance of inductors," *IEEE Transactions on Power Electronics*, vol. 12, no. 4, pp. 671–676, Jul. 1997, doi: 10.1109/63.602562.
- [23] B. Wu, X. Zhang, X. Liu, and C. He, "An analytical model for predicting the self-capacitance of multi-layer circular-section induction coils," *IEEE Transactions on Magnetics*, vol. 54, no. 5, pp. 1–7, May 2018, doi: 10.1109/TMAG.2018.2803771.
- [24] X. Jin, Q. Wang, W. Q. Khan, Z. H. Tang, and X. M. Yao, "Analytical computation of distributed capacitance for NFC coil antenna," *IEICE Electronics Express*, vol. 14, no. 2, 2017, doi: 10.1587/elex.14.20161147.
- [25] M. Kamon, L. Silveira, C. Smithisler, and J. White, "Fasthenry user's guide," *Research Laboratory of Electronics, Department of Electrical Engineering and Computer Science, Massachusetts Institute of Technology*, 1996.
- [26] M. Markovic, "Transmission lines," <https://athena.eecs.csus.edu/~milica/EEE161/lecturenotes/TransmissionLines.pdf> (accessed May 03, 2021).
- [27] J. Ackermann, "Cable velocity factor and loss data (per 100 feet)," *Febo*, 2021. [https://www.febo.com/reference/cable\\_data.html](https://www.febo.com/reference/cable_data.html) (accessed May 03, 2021).

**BIOGRAPHIES OF AUTHORS**

**Yoppy**     received B.Eng. (electrical engineering) from Brawijaya University, Indonesia in 2009. He obtained M.Sc. (embedded systems) from University of Twente, the Netherlands in 2014. He is currently a member of the Applied Electromagnetics research group under the National Research and Innovation Agency (BRIN), Indonesia. His research interests include EMC, power electronics, and embedded systems. He can be contacted at email: yoppy.chia@gmail.com.



**Yudhistira**     is with Research Center for Testing Technology and Standards, National Research and Innovation Agency (BRIN, formerly known as LIPI), Indonesia, from 2014. He received the bachelor degree in Physics from Institut Teknologi Bandung (ITB) from 2007 to 2011 and master degree in electrical engineering at Institut Teknologi Bandung (ITB) from 2018 to 2020. His current research interests in the electromagnetic interference on electrical power systems such as electric vehicles, photovoltaic systems, smart grid, and telecommunication system. He can be contacted at email: yudh013@brin.go.id.



**Hutomo Wahyu Nugroho**     received master (electrical power) degree from Bandung Institute of Technology in 2015. His research interests include electromagnetic measurement, design of system and method EMC test, design and analysis EMC test based on standard. He can be contacted at email: wahjoe.nugroho@gmail.com.



**Elvina Trivida**     received her bachelor degree in physics from Padjadjaran University, Bandung, Indonesia, in 2013 and master degree in engineering physics from Bandung Institute of Technology (ITB), Bandung, Indonesia, in 2016. She is currently a researcher of the Research Center for Testing Technology and Standards under the National Research and Innovation Agency (BRIN), Tangerang Selatan, Indonesia. Her research interests include electronic materials, electromagnetic compatibility, and electromagnetic measurements and applications. She can be contacted at email: elvi004@brin.go.id.



**Tyas Ari Wahyu Wijanarko**     received bachelor degree in physics from Universitas Gadjah Mada, Indonesia in 2016. His research interests include electromagnetic measurements and applications. He can be contacted at email: tyasariwahyu@gmail.com.



**Aditia Nur Bakti**    received the B.S. degree in engineering physics from the Bandung Institute of Technology (ITB), Bandung, Indonesia, in 2008, and Ph.D. degree in science of measurement from the University of Science and Technology (UST), Korea Research Institute of Standards and Science (KRISST) Campus, Daejeon, South Korea, in 2021. He has been a researcher with the Indonesian Institute of Sciences (LIPI) and National Research and Innovation Agency (BRIN), Tangerang Selatan, Indonesia, since 2008 and 2022, respectively. His current research interests include EMC/EMI, antenna measurement, electromagnetic power, and specific absorption rate (SAR) measurement. He can be contacted at email: [adit006@brin.go.id](mailto:adit006@brin.go.id).



**Dwi Mandaris**    received bachelor degree in physics sciences from Institute Technology of Bandung (ITB) Indonesia in 2001 and master degree in electrical engineering at the same University in 2012. He did his Ph.D. in 2020 within Power Electronics and EMC (PE) (before 2018, formerly Telecommunication Engineering, TE Dept) at University of Twente-The Netherlands. Since 2005 until now, he is working as a researcher at Research Center for Testing Technology, National Research and Innovation Agency (BRIN, formerly known as LIPI)-Indonesia. In the last 5 years, he has published many international papers related to EM/EMC. His research interest includes electromagnetic compatibility (EMC) test system, EMI test environments, reverberation chamber (RC), antenna for EMC measurements, EMC simulation and measurement techniques, and telecommunication system. He can be contacted at email: [dwi.mandaris@brin.go.id](mailto:dwi.mandaris@brin.go.id).